The Astrophysical Journal Letters, 711:L117–L121, 2010 March 10 doi:10.1088/2041-8205/711/2/L117

EARLY SOLAR NEBULA CONDENSATES WITH CANONICAL, NOT SUPRACANONICAL, INITIAL $^{26}Al/^{27}Al$ RATIOS

G. J. MacPherson[1], E. S. Bullock[1,6], P. E. Janney[2], N. T. Kita[3], T. Ushikubo[3], A. M. Davis[4], M. Wadhwa[2], and A. N. Krot[5]

[1] Department of Mineral Sciences, National Museum of Natural History, Smithsonian Institution, Washington, DC 20560, USA; macphers@si.edu
[2] School of Earth & Space Exploration & Center for Meteorite Studies, Arizona State University, Tempe, AZ 85287, USA
[3] WiscSIMS, Department of Geoscience, University of Wisconsin-Madison, Madison, WI 53706, USA
[4] Department of the Geophysical Sciences & Enrico Fermi Institute, University of Chicago, Chicago, IL 60637, USA
[5] Hawaii Institute of Geophysics & Planetology, University of Hawaii at Manoa, Honolulu, HI 96822, USA
Received 2008 August 22; accepted 2010 January 20; published 2010 February 23

ABSTRACT

The short-lived radionuclide ^{26}Al existed throughout the solar nebula 4.57 Ga ago, and the initial abundance ratio $(^{26}Al/^{27}Al)_0$, as inferred from magnesium isotopic compositions of calcium–aluminum-rich inclusions (CAIs) in chondritic meteorites, has become a benchmark for understanding early solar system chronology. Internal mineral isochrons in most CAIs measured by secondary ion mass spectrometry (SIMS) give $(^{26}Al/^{27}Al)_0 \sim (4–5) \times 10^{-5}$, called "canonical." Some recent high-precision analyses of (1) bulk CAIs measured by multicollector inductively coupled plasma mass spectrometry (MC-ICPMS), (2) individual CAI minerals and their mixtures measured by laser-ablation MC-ICPMS, and (3) internal isochrons measured by multicollector (MC)-SIMS indicated a somewhat higher "supracanonical" $(^{26}Al/^{27}Al)_0$ ranging from $(5.85 \pm 0.05) \times 10^{-5}$ to $>7 \times 10^{-5}$. These measurements were done on coarse-grained Type B and Type A CAIs that probably formed by recrystallization and/or melting of fine-grained condensate precursors. Thus the supracanonical ratios might record an earlier event, the actual nebular condensation of the CAI precursors. We tested this idea by performing in situ high-precision magnesium isotope measurements of individual minerals in a fine-grained CAI whose structures and volatility-fractionated trace element abundances mark it as a primary solar nebula condensate. Such CAIs are ideal candidates for the fine-grained precursors to the coarse-grained CAIs, and thus should best preserve a supracanonical ratio. Yet, our measured internal isochron yields $(^{26}Al/^{27}Al)_0 = (5.27 \pm 0.17) \times 10^{-5}$. Thus our data do not support the existence of supracanonical $(^{26}Al/^{27}Al)_0 = (5.85–7) \times 10^{-5}$. There may not have been a significant time interval between condensation of the CAI precursors and their subsequent melting into coarse-grained CAIs.

Key words: astrochemistry – nuclear reactions, nucleosynthesis, abundances – protoplanetary disks

1. INTRODUCTION

The presence of the short-lived ($t_{1/2} = 0.73$ Myr) radionuclide ^{26}Al in the early solar system is well established (Lee et al. 1976; MacPherson et al. 1995), but the abundance of ^{26}Al relative to stable ^{27}Al at the time of solar system birth ("initial" $^{26}Al/^{27}Al$, or $(^{26}Al/^{27}Al)_0$) is the subject of renewed debate. The question is important for two reasons. First, ^{26}Al may have been a major heat source for early planetary melting and differentiation. Second, $(^{26}Al/^{27}Al)_0$ represents "time zero" for a high-resolution relative chronometer of closely spaced events that occurred at ~4.57 Ga, the birth of the solar system.

Evidence for extinct ^{26}Al, as excesses of its decay product ^{26}Mg, is found in primordial solar system materials that are preserved in chondritic meteorites and interplanetary dust particles. The highest inferred $^{26}Al/^{27}Al$ ratios occur in calcium–aluminum-rich inclusions (CAIs), which are the earliest solar system solids and which define $(^{26}Al/^{27}Al)_0$. Lower inferred ratios are found in objects such as chondrules, which thus probably formed later than CAIs (Krot et al. 2009 and references therein).

Internal mineral isochrons measured in CAIs by secondary ion mass spectrometry (SIMS) over the past ~30 years have yielded a relatively consistent ("canonical") range of $(^{26}Al/^{27}Al)_0 \sim (4–5) \times 10^{-5}$ (MacPherson et al. 1995). Since the development of multicollection techniques for both SIMS and laser-ablation inductively coupled plasma mass spectrometry (LA-ICPMS), there have been several reports of "supracanonical" isochrons yielding $(^{26}Al/^{27}Al)_0$ up to 7×10^{-5} (Taylor et al. 2005; Young et al. 2005; Cosarinsky et al. 2007), but none is unambiguous (see the discussion). Two recent studies (Bizzarro et al. 2005; Thrane et al. 2006) reported $(^{26}Al/^{27}Al)_0 = (5.85 \pm 0.05) \times 10^{-5}$, based on a whole-rock isochron from high-precision magnesium isotope and Al/Mg analyses of *bulk* CAIs. Because this whole-CAI supracanonical value differs from those generally determined from internal mineral isochrons, it has been asserted (e.g., Thrane et al. 2006) that the supracanonical value records the time of primary aluminum–magnesium chemical fractionation during nebular condensation of the CAI precursors. According to this model, the canonical value $(^{26}Al/^{27}Al)_0 \sim (4–5) \times 10^{-5}$ determined from internal isochrons records only the time that each CAI was last melted or otherwise reprocessed (Thrane et al. 2006; Young et al. 2005); thus, the true "time zero" should be based on $(^{26}Al/^{27}Al)_0 = (5.85 \pm 0.05) \times 10^{-5}$. One obvious test of this hypothesis is to locate and analyze samples of the precursors to CAIs, i.e., primary nebula condensates. Nebular condensates exist, in the form of fine-grained, spinel-rich CAIs from reduced CV3 chondrites such as Leoville and Efremovka. These distinctive CAIs have complex and delicately layered structures that are not compatible with an igneous origin (Krot et al. 2004). Their defining characteristic is a volatility-fractionated trace-element pattern ("Group II") that can only be explained by high-temperature

[6] Present address: Department of the Geophysical Sciences, University of Chicago, Chicago, IL 60637, USA.

Table 1
Al–Mg isotope systematics in Leoville 3536-1

No.	$^{27}Al/^{24}Mg$ ($\pm 2\sigma$)	$\delta^{25}Mg$ (‰, $\pm 2\sigma$)	$\delta^{26}Mg^{*a}$ (‰, $\pm 2\sigma$)	Phases/fractions	Method
1	1.25 ± 0.05	−2.51 ± 0.05	0.54 ± 0.14	Sp30; Pyx62; Plag8	ICPMS
2	7.57 ± 0.23	0.79 ± 0.09	2.73 ± 0.29	Sp7; Pyx3; Mel79; Plag11	ICPMS
3	3.60 ± 0.10	−1.17 ± 0.05	1.55 ± 0.18	Sp25; Pyx9; Mel61; Plag5	ICPMS
4	5.06 ± 0.06	−0.95 ± 0.07	2.08 ± 0.21	Sp26; Pyx6; Mel58; Plag10	ICPMS
5	3.77 ± 0.04	−3.51 ± 0.08	1.52 ± 0.26	Sp22; Pyx20; Mel0; Plag57	ICPMS
6	2.64 ± 0.04	−3.09 ± 0.06	1.01 ± 0.16	Sp39; Pyx27; Plag34	ICPMS
7	2.41 ± 0.04	−3.11 ± 0.06	1.13 ± 0.20	Sp25; Pyx32; Mel6; Plag38	ICPMS
8	3.63 ± 0.06	−1.83 ± 0.06	1.42 ± 0.17	Sp38; Pyx12; Mel27; Plag23	ICPMS
9	2.28 ± 0.06	−2.84 ± 0.05	0.75 ± 0.15	Sp12; Pyx40; Mel20; Plag28	ICPMS
10	1.35 ± 0.06	−2.92 ± 0.09	0.47 ± 0.25	Sp19; Pyx53; Mel4; Plag24	ICPMS
11	3.95 ± 0.07	−2.14 ± 0.06	1.37 ± 0.19	Sp13; Pyx21; Mel40; Plag26	ICPMS
12	38.03 ± 0.22	−1.4 ± 1.0	14.7 ± 1.6	Mel	SIMS
13	23.45 ± 0.13	−1.4 ± 0.8	9.0 ± 1.1	Mel	SIMS
14	40.65 ± 0.30	−0.6 ± 0.7	15.1 ± 1.1	Mel	SIMS
15	23.97 ± 0.07	−0.5 ± 0.5	9.5 ± 0.8	Mel	SIMS
16	41.08 ± 0.39	−0.6 ± 0.7	15.1 ± 1.0	Mel	SIMS
17	36.58 ± 0.25	−1.1 ± 0.6	13.8 ± 0.9	Mel	SIMS
18	18.92 ± 0.04	−1.6 ± 0.9[b]	6.7 ± 1.3	Mel	SIMS
19	2.64 ± 0.03	−0.35 ± 0.13[b]	1.02 ± 0.20	Sp	SIMS
20	2.62 ± 0.03	−0.10 ± 0.13[b]	1.02 ± 0.20	Sp	SIMS
21	0.321 ± 0.003	−2.09 ± 0.15[b]	−0.14 ± 0.24	Pyx	SIMS

Notes.
[a] $\delta^{26}Mg^*$ is $\delta^{26}Mg$ corrected for mass fractionation using $\delta^{25}Mg$ and an exponent of 0.514 (see the text). [b] $\delta^{25}Mg$ for spinel and pyroxene are obtained by assuming that the terrestrial standards are not fractionated. Mel: melilite; Plag: plagioclase; Pyx: pyroxene; Sp: spinel; ICPMS: inductively coupled plasma mass spectrometry; SIMS: secondary ion mass spectrometry.

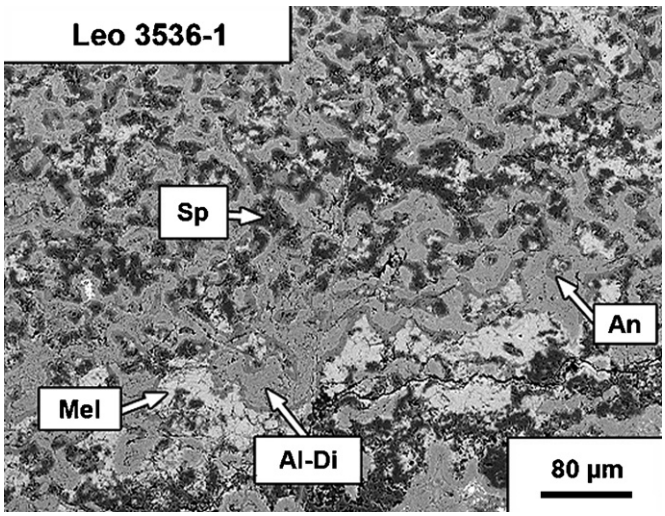

Figure 1. Backscattered electron image of the Leoville CAI 3536-1. Irregular patches of spinel (Sp) and melilite (Mel) are mantled by semicontinuous layers of aluminous diopside (Al-Di) and anorthite (An).

fractional condensation of the nebular gas (Boynton 1975; Davis & Grossman 1979). Because they preserve intact the unmistakable chemical and textural imprints of actual condensation, these fine-grained CAIs should preserve the initial $^{26}Al/^{27}Al$ ratios at the time of condensation. Thus they are ideal candidates on which to test the supracanonical model. The small grain sizes of such objects (typically $\leqslant \sim 10\,\mu m$) have made isotopic studies difficult in the past, but the greater sensitivity of the newest generation of SIMS instruments has enabled smaller beam spots to be used to acquire high-precision data.

We measured magnesium isotopes in one fine-grained, spinel-rich CAI from the Leoville CV3 chondrite, labeled Leoville 3536-1 (Figure 1; analyzed and described by Mao et al. 1990 and Krot et al. 2004), whose somewhat larger average grain size than most similar objects makes it particularly amenable to high-precision microbeam isotopic analysis. It consists entirely of the primary high-temperature phases melilite, spinel, anorthite, and aluminous diopside; it is devoid of alkali- and halogen-bearing secondary phases that are abundant in Allende CAIs.

We used both laser-ablation multicollector inductively coupled plasma mass spectrometry (LA-MC-ICPMS; see Appendix A) and IMS-1280 large radius SIMS (see Appendix B). The LA-MC-ICPMS analyses were collected using a $\sim 90\,\mu m$ laser spot size which, for such a fine-grained object, resulted in multiple mineral grains within each spot. The modal mineralogy of each laser spot was determined using image analysis of backscattered electron (BSE) images and element X-ray area maps taken with a scanning electron microscope (SEM). The SIMS analyses utilized $7\,\mu m$ beam spots for melilite and $12\,\mu m$ beam spots for spinel and pyroxene, thus permitting analysis of a single phase within most spots.

2. ISOTOPIC COMPOSITIONS

The aluminum–magnesium isotopic data for Leoville 3536-1 are given in Table 1 and plotted on an isochron diagram in Figure 2. The LA-ICPMS data for multi-mineral spots define a correlation line between $^{26}Mg/^{24}Mg$ versus $^{27}Al/^{24}Mg$ corresponding to $(^{26}Al/^{27}Al)_0 = (5.25 \pm 0.86) \times 10^{-5}$, with an intercept (initial $\delta^{26}Mg$) of 0.06‰ ± 0.21‰, MSWD = 1.8, and $^{27}Al/^{24}Mg$ values up to ∼7.6. Because of the low $^{27}Al/^{24}Mg$ values, the slope of the LA-ICPMS isochron is not resolved from those of either the canonical ($\sim 5 \times 10^{-5}$) or supracanonical $(5.85 \pm 0.05) \times 10^{-5}$ ones. However, the SIMS data for individual mineral phases extend to much higher $^{27}Al/^{24}Mg$ values (up to 45) and define a precise correlation line yielding $(^{26}Al/^{27}Al)_0 = (5.29 \pm 0.18) \times 10^{-5}$, initial

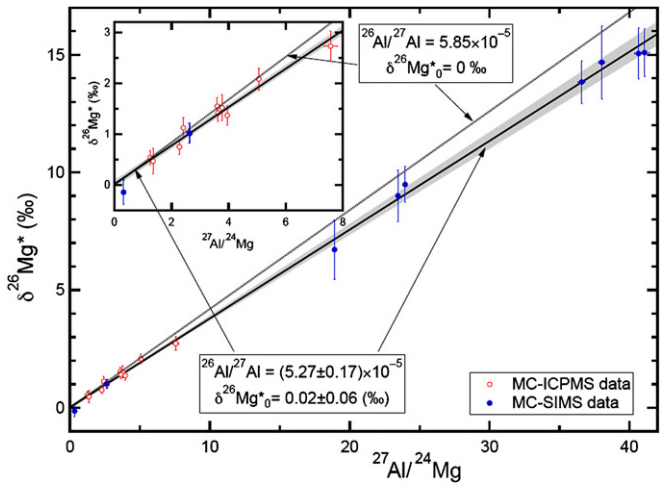

Figure 2. Magnesium isotope data for the Leoville CAI 3536-1. All data show an excellent linear correlation of $\delta^{26}Mg$ with $^{27}Al/^{24}Mg$. The initial $^{26}Al/^{27}Al$ calculated from a weighted least-squares fit to all of the data (shown) is clearly resolved from the "supracanonical" value of 5.85×10^{-5} and within error of the canonical value of 5×10^{-5}. The inset is an enlargement of the region at low $^{27}Al/^{24}Mg$.

$\delta^{26}Mg = -0.05‰ \pm 0.13‰$, and MSWD = 0.9. The smaller error on the slope of the SIMS-based isochron is due to the higher $^{27}Al/^{24}Mg$ values relative to the LA-ICPMS data. The combined data sets are within error of one another, and define a correlation line (MSWD = 1.3) yielding $(^{26}Al/^{27}Al)_0 = (5.27 \pm 0.17) \times 10^{-5}$, initial $\delta^{26}Mg = 0.02‰ \pm 0.06‰$, and MSWD = 1.3. The initial $^{26}Al/^{27}Al$ ratio of Leoville 3536-1 is clearly resolved from the supracanonical value of $(5.85 \pm 0.05) \times 10^{-5}$ (Thrane et al. 2006).

3. IMPLICATIONS: CANONICAL VERSUS SUPRACANONICAL INITIAL $^{26}AL/^{27}AL$ RATIOS

CAIs are the oldest objects formed in the solar system (Amelin et al. 2002), and preserve the highest measured value for initial $^{26}Al/^{27}Al$ (excepting presolar grains). This canonical ratio for initial $^{26}Al/^{27}Al$ is chronologically important because it marks the approximate time of solar system birth. However, the exact value of the ratio is less precisely defined than is commonly assumed. MacPherson et al. (1995) compiled all data then available for $(^{26}Al/^{27}Al)_0$ in early solar system materials and showed a histogram of these values, in which most CAI data define a peak centered on 4.5×10^{-5}. Accordingly, some authors have defined canonical $(^{26}Al/^{27}Al)_0$ to be 4.5×10^{-5}. But the histogram peak has substantial width, mostly in the range $(3.2–5.5) \times 10^{-5}$, due at least in part to analytical uncertainties in the data at that time (*especially for data having low Al/Mg ratios*). Therefore, MacPherson et al. (1995) specifically did not define the canonical value based on the histogram peak center. Instead, they recommended the value of 5×10^{-5} as a reasonable *approximate* upper limit, because many analyzed phases with $^{27}Al/^{24}Mg > 1200$ have initial $^{26}Al/^{27}Al \sim 5 \times 10^{-5}$ but *none* are significantly above it. Recent high-precision bulk CAI data (Jacobsen et al. 2008) give a slightly higher value of $(5.23 \pm 0.13) \times 10^{-5}$ ($\pm 2\sigma$). We accept the latter value as canonical for the purposes of the following discussion, and the importance here has to do with whether some recently reported supracanonical values really are higher than canonical.

The putative existence of $(^{26}Al/^{27}Al)_0 = \sim 6 \times 10^{-5}$ preserved in *some* CAI material, relative to the lower "canonical" ratios generally inferred from internal CAI isochrons, implies the interesting possibility that a measurable time gap existed between condensation of the CAI precursors and the final crystallization of the CAIs themselves. The evidence for the higher ratio comes from two types of data: in situ analyses from a number of CAIs, using high-precision SIMS and LA-ICPMS techniques, and analyses of bulk CAIs.

The in situ data (Young et al. 2005; Taylor et al. 2005; Cosarinsky et al. 2007) were interpreted to be the *partially* preserved remnants of internal supracanonical isochrons. Cosarinsky et al. (2007; who incorporated the data of Taylor et al. 2005) analyzed (via SIMS) only phases with very low $^{27}Al/^{24}Mg$ ratios (spinel and aluminous diopside), on the assumption that high Al/Mg phases such as melilite and anorthite may have been partially reset. They also forced their regressions to pass through the origin, which may not be a safe assumption (e.g., note that Thrane et al. 2006, who advocate supracanonical $(^{26}Al/^{27}Al)_0$, do not force their regressions through the origin). However, other recent high-precision in situ SIMS studies that specifically *include* melilite and anorthite (Kita et al. 2007, 2008; Makide et al. 2009) have yielded well-defined isochrons with only canonical ratios. Connolly et al. (2009) used high-precision SIMS and LA-ICPMS both on the same CAI and showed that both techniques yield similar supracanonical results for some melilite grains at low $^{27}Al/^{24}Mg$, but anorthite in the same CAI is disturbed and thus the origin of the "supracanonical" melilite values remains open to question. Young et al. (2005) used LA-ICPMS to obtain data for several CAIs, and nearly 79% of their analyses yielded apparent supracanonical $(^{26}Al/^{27}Al)_0$ relative to the histogram peak value of 4.5×10^{-5}. However, relative to $(^{26}Al/^{27}Al)_0 = 5 \times 10^{-5}$, that percentage drops to just over 50%. One highlighted inclusion (Leoville 144A) yielded $(^{26}Al/^{27}Al)_0 = (5.9 \pm 0.3) \times 10^{-5}$ ($\pm 2\sigma$). However, the data for this object show significant scatter on the isochron diagram (MSWD = 3.3) that likely indicates isotopic disturbance. Moreover, the relatively large laser spot size (50–100 μm) used to acquire their LA-ICPMS data prevented obtaining any analyses with high $^{27}Al/^{24}Mg$. Together these factors preclude a precise estimate of the true initial $^{26}Al/^{27}Al$ ratio at the time Leoville 144A formed. Another contributing factor to the uncertainty over whether their data are resolved from canonical rests on their use of the value 0.521 for the mass fractionation correction factor, β, for calculating the radiogenic component of excess ^{26}Mg in their analyses. Davis et al. (2005) argued that $\beta = 0.521$ is ill suited for low-Al/Mg phases in CAIs that show (and many do) significant intrinsic mass-dependent isotopic fractionation of magnesium, and recommended a value for $\beta = 0.514$ based on isotopic measurements of laboratory-produced evaporation residues. By using $\beta = 0.514$ instead of 0.521 to correct for mass fractionation, the inferred initial $^{26}Al/^{27}Al$ ratio of CAI 144A decreases from $(5.9 \pm 0.3) \times 10^{-5}$ to $(5.6 \pm 0.42) \times 10^{-5}$, which is not resolved from $(5.23 \pm 0.13) \times 10^{-5}$. Lastly, Leoville 144A is a compact Type A CAI, which by virtue of being probably once molten is one of the very objects least expected by the model of Young et al. (2005) to preserve any evidence for supracanonical $(^{26}Al/^{27}Al)_0$.

Thus, the principal evidence for a supracanonical $(^{26}Al/^{27}Al)_0$ ratio of $\sim 6 \times 10^{-5}$ rests with the bulk CAI data (whole rock isochrons) of Bizzarro et al. (2005)[7] and Thrane et al.

[7] The original paper by Bizzarro et al. (2004) reported only canonical initial ratios.

(2006) and which, according to the model of those authors, are independent of whether any of their CAIs have canonical internal isochrons, because the latter presumably reflect only the time of final solidification.

Their results, however, have proven to be controversial. Subsequent studies of bulk CAIs, using techniques similar to those of Bizzarro et al. (2005) and Thrane et al. (2006), have not reproduced supracanonical initial ratios. Jacobsen et al. (2008) in particular carefully validated both the magnesium isotopic analyses and the measurements of Al/Mg in several ways, and obtained canonical $(^{26}Al/^{27}Al)_0 = (5.23 \pm 0.13) \times 10^{-5}$. Baker (2008) obtained results in close agreement with those of Jacobsen et al. (2008).

The reasons for the discrepancy between the results of Thrane et al. (2006) and more recent data (Jacobsen et al. 2008; Baker 2008) are not yet understood. Nevertheless, the principal rationale for our study was to find the best example of an *un*processed CAI, one that formed by primary condensation, because such an object would represent the best possibility of finding a well-defined supracanonical internal isochron. Leoville 3536-1 has both the petrologic and chemical signatures of a condensate, and yet our isotopic data define an undisturbed isochron that yields canonical $(^{26}Al/^{27}Al)_0$, $(5.27 \pm 0.17) \times 10^{-5}$.

The difference between our results and those of Bizzarro et al. (2005) and Thrane et al. (2006) cannot be explained as due to reprocessing or recrystallization of Leoville 3536-1 or other fine-grained CAIs (cf. Young et al. 2005). But such CAIs certainly never have been melted: had they been, their anorthite-normative bulk compositions would result in distinctive igneous (ophitic) textures (characteristic of, e.g., Type C CAIs; Tronche et al. 2007). Krot et al. (2004) noted that the melilite-rich mantles of fine-grained CAIs such as Leoville 3536-1 are difficult to explain by single-stage condensation, and might have formed as a result of later reheating accompanied by evaporation. But the isotopically light magnesium compositions of the melilite-rich mantle and anorthite-rich core of the Leoville 3536-1 (Table 1) indicate that the mantle could not have resulted from melt evaporation (Richter 2004). Moreover, even solid-state evaporation cannot explain the melilite mantles, as those mantles have higher Si/Al and Mg/Al relative to the cores—opposite what would be expected. Also, our δ^{25}Mg data (both SIMS and ICPMS) are isotopically light (negative; Table 1) in the melilite mantles just as in the cores, indicating that the mantles also formed by condensation (e.g., Niederer and Papanastassiou, 1984), possibly from a gas of non-solar composition.

One plausible way to reconcile our data with those of Bizzarro et al. (2005) and Thrane et al. (2006) is the possibility that fine-grained, spinel-rich CAIs with Group II trace element patterns are a different, younger breed of CAI arising from a later episode of condensation subsequent to the hypothetical *primordial* condensates. This requires the special coincidence that Group II CAIs were condensing at precisely the same time as the Types A and B CAIs were being processed. There admittedly are no absolute age data to show that fine-grained spinel-rich CAIs are older (or younger) than any other CAIs, but the nature of the volatility-controlled Group II trace element pattern argues against their being younger. The Group II signature, which is understood primarily in terms of volatility-controlled fractionation of the rare earth elements (REE), reflects fractional condensation from gas to solid (Boynton, 1975; Davis & Grossman, 1979). Condensation of a very high temperature phase (likely hibonite, $CaAl_{12}O_{19}$; MacPherson & Davis 1994) selectively incorporates the most refractory REE into the condensing solids and leaves the more volatile REE in the gas. Subsequent condensation from the remaining reservoir will produce phases depleted in those most refractory REE and relatively enriched in the more volatile REE, i.e., the Group II pattern. However, even Group II patterns are depleted in the two most volatile REE, europium and ytterbium. Most CAIs, especially in CV3 chondrites, have relatively unfractionated REE patterns: they are uniformly enriched in both refractory and volatile REE (including europium and ytterbium), meaning that they represent condensation of the REE to lower temperatures than do the Group II patterns. In the sense that lower temperatures correspond to a later time, the unfractionated "normal" CAIs are relatively younger than the CAIs with Group II trace element patterns, not the other way around. This is further supported by the observation that some coarse-grained CAIs have Group II trace element patterns (e.g., Wark 1987), suggesting that those inclusions formed by melting of fine-grained precursors with the Group II trace element patterns. Finally, fine-grained spinel-rich inclusions like Leoville 3536-1 have subchondritic bulk Ca/Al ratios, so they cannot have recondensed from vapor that was fractionally evaporated from an earlier generation of CAIs or CAI precursors. Such vapor would be depleted, not enriched, in aluminum.

We find no compelling arguments that Leoville 3536-1 and its kin are anything other than primordial condensates. Thus our data do not support the existence of supracanonical $(^{26}Al/^{27}Al)_0$: we analyzed a type of CAI that should best preserve it yet we find only canonical $(^{26}Al/^{27}Al)_0$. The existence of supracanonical initial $^{26}Al/^{27}Al$ in the solar system will remain in doubt until convincing internal mineral isochrons unaffected by local re-equilibration are found that clearly indicate such ratios.

Leoville 3536-1 records the time of the condensation event that formed this particular inclusion. The data of Jacobsen et al. (2008) record the time of high-temperature Mg/Al fractionation of a suite of whole CAIs. These two events are contemporaneous within analytical uncertainty. Moreover, both are approximately contemporaneous with the melting event recorded by a coarse-grained igneous CAI measured by our group (e.g., Kita et al. 2008). Collectively, these observations indicate that nebular Mg/Al fractionation, condensate CAI formation, and melting of some CAIs occurred within a very short time interval, perhaps only a few tens of thousands of years.

This work was supported by NASA grants NNX07AJ05G (G.J.M.), NNX07AI46G (N.K.), NNG06GE52G (M.W.), NNG06-GF19G and NNX09-AG39G (A.M.D.), and NAG5-10610 (A.N.K.). Wisc-SIMS is supported partly by NSF (EAR03-19230 and EAR07-44079, PI: J. W. Valley). Detailed comments by three anonymous reviewers led to improvements in the manuscript.

APPENDIX A

LA-MC-ICPMS measurements were made at the Field Museum in Chicago using a GV Instruments IsoProbe with a New Wave UP193HE excimer laser ablation system. The mass spectrometer was run at a mass-resolving power of approximately 400, and with a slight positive voltage applied to the extraction lens to minimize magnesium background intensities to $<5 \times 10^{-15}$ A. Individual measurements consisted of 20 integration cycles (7 s each). The laser spot size was 90 μm, with a repeat rate of 4 Hz and a laser energy density of $\sim$2 J cm^{-2}.

Signal intensities for ^{24}Mg ranged from 0.6 to 3.0 $\times$ 10^{-11} A. All measurements employed sample-standard bracketing. Standards were isotopically well-characterized synthetic glasses from evaporation experiments having CAI-like compositions (Richter et al. 2007), chosen to approach the composition of the unknown analyzed phase assemblage. Based on the analyses of these glasses, external reproducibilities (2σ) for our measurements are $\pm$0.20‰ for $\delta^{26}Mg$. Internal precisions of individual measurements of unknowns typically are larger, $\pm$0.3‰–1.3‰ for $\delta^{26}Mg$, because it was not possible to make repeat measurements of the same spot. Both natural and instrumental mass fractionation were corrected using an exponential law with $\beta = 0.514$ (Davis et al. 2005).

Analyses of terrestrial mineral standards (diopside, spinel, and gehlenitic melilite) showed no resolvable excesses or deficits in $\delta^{26}Mg$ that would indicate that our CAI $\delta^{26}Mg$ data were affected by matrix effects or isobaric interferences. Specifically, we observed no significant contribution of $^{48}Ca^{++}$ to the $^{24}Mg^{+}$ signal in melilite (Ca-rich); this is not surprising given the low isotopic abundance of ^{48}Ca (0.19%). We made one additional test to evaluate the potential effect of $^{48}Ca^{++}$ to the $^{24}Mg^{+}$ signal, by ablating calcite and scanning over the mass range of 21 amu to 22 amu to determine if there was any $^{43}Ca^{++}$ present at 21.5 amu. The isotopic abundance of ^{43}Ca (0.14%) is similar to that of ^{48}Ca (0.19%), and if any appreciable $^{48}Ca^{++}$ were produced, we would have expected to see a signal at mass 21.5 amu. We observed no signal above background at this mass. It is likely that thermalization of the ion beam (from collisions with neutral gas atoms) in the hexapole collision cell of the IsoProbe MC-ICPMS effectively eliminates doubly charged ions.

APPENDIX B

The large radius SIMS CAMECA IMS 1280 at the University of Wisconsin-Madison (Wisc-SIMS) was used to obtain high-precision/high spatial resolution magnesium isotopic analyses. The primary beam was O^{-}, operated under conditions similar to those described in Kita et al. (2000). Two different analytical conditions were used. Melilite ($^{27}Al/^{24}Mg > 10$) was analyzed using a 3 $\times$ 7 μm beam spot (0.1 nA intensity) in order to avoid grain boundaries with magnesium-rich phases; magnesium isotope signals were detected with a monocollection electron multiplier pulse-counting system in magnetic peak jumping mode, at a mass-resolving power of 3500. Spinel and pyroxene ($^{27}Al/^{24}Mg < 10$) were analyzed using a $\sim$10 $\times$ 15 μm beam (1.4 nA intensity) with multicollector Faraday Cup (MCFC) detectors to achieve high precision ($\leqslant$0.2‰) at a mass-resolving power of 2200. ^{27}Al signals were collected on a MCFC detector simultaneously with Mg isotopes in both cases. The standards used to correct instrumental bias on the magnesium isotope analyses were synthetic zoned melilite crystals, glass, spinel, and pyroxene. Both natural and instrumental mass fractionation were corrected using an exponential law with $\beta = 0.514$ (Davis et al. 2005). Secondary ^{24}Mg intensities typically were 1 $\times$ 10^{5} cps for melilite (MgO $<$ 2%), and 4 $\times$ 10^{7} cps for spinel and pyroxene (MgO $\sim$ 20%). The dead time of the monocollection electron multiplier detector was estimated to be 20.4 $\pm$ 1.8 (2σ) ns from the analyses of standards with various Mg intensities (5 $\times$ 10^{4}–3 $\times$ 10^{5} cps). External reproducibilities (2σ) for $\delta^{26}Mg^{*}$ were $\sim$1‰ for melilite analyses and $\leqslant$0.2‰ for spinel and pyroxene analyses. During some melilite analyses, the Mg^{+} intensity increased significantly during analyses because of μm-size magnesium-rich phases. We rejected all such data. Similarly, we rejected any analyses that hit mixed phases, based on SEM examination of all SIMS spots.

REFERENCES

Amelin, Y., Krot, A. N., Hutcheon, I. D., & Ulyanov, A. A. 2002, Science, 297, 1678
Baker, J. A. 2008, Geochim. Cosmochim. Acta, 72, A45
Bizzarro, M., Baker, J. A., & Haack, H. 2004, Nature, 431, 275
Bizzarro, M., Baker, J. A., & Haack, H. 2005, Nature, 435, 1280
Boynton, W. V. 1975, Geochim. Cosmochim. Acta, 39, 569
Connolly, H. C., Jr., et al. 2009, Lunar Planet. Sci., 40, 1993
Cosarinsky, M., Taylor, D. J., Liu, M.-C., McKeegan, K. D., & Krot, A. N. 2007, in Workshop on the Chronology of Meteorites and the Early Solar System, LPI Contribution No. 1374, 48
Davis, A. M., & Grossman, L. 1979, Geochim. Cosmochim. Acta, 43, 1611
Davis, A. M., Richter, F. M., Mendybaev, R. A., Janney, P. E., Wadhwa, M., & McKeegan, K. D. 2005, Lunar Planet. Sci., 36, 2334
Jacobsen, B., Yin, Q.-Z., Moynier, F., Amelin, Y., Krot, A. N., Nagashima, K., Hutcheon, I. D., & Palme, H. 2008, Earth Planet. Sci. Lett., 272, 353
Kita, N. T., Nagahara, H., Togashi, S., & Morishita, Y. 2000, Geochim. Cosmochim. Acta, 64, 3913
Kita, N. T., Ushikubo, T., Fournelle, J., Knight, K. B., Mendybaev, R. A., Davis, A. M., & Richter, F. M. 2008, Geochim. Cosmochim. Acta, 72, A477
Kita, N. T., Ushikubo, T., Knight, K. B., Mendybaev, R. A., Davis, A. M., & Richter, F. M. 2007, in Workshop on Chronology of Meteorites and the Early Solar System, LPI Contribution No. 1374, 92
Krot, A. N., MacPherson, G. J., Ulyanov, A. A., & Petaev, M. I. 2004, Meteorit. Planet. Sci., 39, 1517
Krot, A. N., et al. 2009, Geochim. Cosmochim. Acta, 73, 4963
Lee, T., Papanastassiou, D. A., & Wasserburg, G. J. 1976, Geophys. Res. Lett., 3, 109
MacPherson, G. J., & Davis, A. M. 1994, Geochim. Cosmochim. Acta, 58, 5599
MacPherson, G. J., Davis, A. M., & Zinner, E. K. 1995, Meteorit. Planet. Sci., 30, 365
MacPherson, G. J., Simon, S. B., Davis, A. M., Grossman, L., & Krot, A. N. 2005, in ASP Conf. Ser. 341, Chondrites and the Protoplanetary Disk, ed. A. N. Krot, E. R. D. Scott, & B. Reipurth (San Francisco, CA: ASP), 225
Makide, K., Nagashima, K., Krot, A. N., Huss, G. R., Hutcheon, I. D., & Bischoff, A. 2009, Geochim. Cosmochim. Acta, 73, 5018
Mao, X.-Y., Ward, B. J., Grossman, L., & MacPherson, G. J. 1990, Geochim. Cosmochim. Acta, 54, 2121
Niederer, F. R., & Papanastassiou, D. A. 1984, Geochim. Cosmochim. Acta, 48, 1279
Podosek, F. A., Zinner, E. K., MacPherson, G. J., Lundberg, L., Brannon, J. C., & Fahey, A. J. 1991, Geochim. Cosmochim. Acta, 55, 1083
Richter, F. M. 2004, Geochim. Cosmochim. Acta, 68, 4971
Richter, F. M., Janney, P. E., Mendybaev, R. A., Davis, A. M., & Wadhwa, M. 2007, Geochim. Cosmochim. Acta, 71, 5544
Taylor, D. J., Cosarinsky, M., Liu, M.-C., McKeegan, K. D., Krot, A. N., & Hutcheon, I. D. 2005, Meteorit. Planet. Sci., 40, A151
Thrane, K., Bizzarro, M., & Baker, J. A. 2006, ApJ, 646, L159
Tronche, E. J., Hewins, R. H., & MacPherson, G. J. 2007, Geochim. Cosmochim. Acta, 71, 3361
Wark, D. A. 1987, Geochim. Cosmochim. Acta, 51, 221
Young, E. D., Galy, A., & Nagahara, H. 2002, Geochim. Cosmochim. Acta, 66, 1095
Young, E. D., Simon, J. I., Galy, A., Russell, S. S., Tonui, E., & Lovera, O. 2005, Science, 308, 223